An Approach to Telerobotic Manipulations

H. Kazerooni

C. L. Moore[1]

Mechanical Engineering Department,
University of California,
5124 Etcheverry Hall,
Berkeley, CA 95720

This article introduces three areas of study: 1 telefunctioning; 2 a control method for producing telefunctioning; and 3 an analysis of human-robot interaction when telefunctioning governs the system behavior. Telefunctioning facilitates the maneuvering of loads by creating a perpetual sense of the load dynamics for the operator. Telefunctioning is defined as a robotic manipulation method in which the dynamic behaviors of the slave robot and the master robot are functions of each other; these functions are the designer's choice and depend on the application. (In a subclass of telefunctioning currently referred to as telepresence, these functions are specified as "unity" so that the master and slave variables (e.g., position, velocity) are dynamically equal.) To produce telefunctioning, this work determines a minimum number of functions relating the robots' variables, and then develops a control architecture which guarantees that the defined functions govern the dynamic behavior of the closed-loop system. The stability of the closed-loop system (i.e., master robot, slave robot, human, and the load being manipulated) is analyzed and sufficient conditions for stability are derived.

1 Definition of Telefunctioning

A telerobotic system consists of two robots: the master which is maneuvered by a human, and the slave which performs a task at a location remote from the master. The master robot is not connected mechanically to the slave robot. Figure 1 shows a telerobotic system where a human is pushing against the master and the slave is pushing against an environment.[2] "Telepresence" denotes a dynamic behavior in which the environmental effects experienced by the slave are transferred through the master to the human without alteration; therefore, the human feels that she/he is "there" without "being" there [2, 3, 6, 16, 20]. The following three examples discuss the concept of telefunctioning and how it differs from telepresence.[3]

Example 1. Suppose a telerobotic system is used to manipulate an object through a completely arbitrary trajectory. The goal may be a dynamic behavior in which the human senses scaled-down values of the forces that the slave senses when manipulating the object. Therefore, a system controller must be designed so that the ratio of the forces on the slave to the forces on the master equals a number greater than unity. If f_S and f_M[4] represent the forces on the slave and on the master, then $f_S = -\alpha f_M$ where α is a scalar greater than unity. (The negative sign, originating from the convention used in Fig. 1, implies the opposite directions of f_S and f_M.)

Furthermore, if the object being manipulated is a pneumatic jackhammer, the goal may be to both filter and decrease the jackhammer forces. Then, the human senses only the low-frequency, scaled-down components of the forces that the slave senses. This requires a low-pass filter such that $f_S = -\alpha f_M$ where $1/\alpha$ is a low-pass filter transfer function.

In this example of telefunctioning, the slave forces are functions of the master forces so the human senses forces different from those which the slave senses. In general, the slave and master forces are not equal as they would be in the case of telepresence.

Example 2. In maneuvers over an arbitrary trajectory, the goal may be a dynamic behavior for the telerobotic system in which the human, who is maneuvering a rigid body, feels the forces as being those of maneuvering a light single-point mass. This dynamic behavior masks the cross-coupled forces associated with maneuvering a rigid body; the human feels only the forces associated with the acceleration of a single-point mass. This behavior is desirable because cross-coupled forces contribute to the difficulty of maneuvering a rigid body. In contrast to this telefunctioning example, when telepresence governs the system behavior, the forces on the master robot and slave robot are equal, and the human would feel all of the forces, including the cross-coupled forces, associated with maneuvering a rigid body.

For the example above, the relationship between the forces on the master robot and the forces on the slave robot cannot be given explicitly by an equation. Later, a mathematical tool is developed to frame the design specifications needed in this situation.

Example 3. In maneuvers over an arbitrary trajectory, the goal may be a behavior for the telerobotic system in which the slave robot position (not force, as in example 1) equals a scaled-down value of the master robot position. In other words, if y_S and y_M are the positions of the slave robot and the master robot, then $y_S = \beta y_M$ where β is smaller than unity. This behavior is useful when great precision is required in the slave maneuver; a few centimeters of master motion correspond to a few microns of slave motion. This would have applications in microsurgery. In contrast to this telefunctioning example, when telepresence governs the system behavior, y_S and y_M are equal.

In each of the above examples, one relationship between the master robot and slave robot variables is chosen as the performance specification for telefunctioning. But, several independent relationships might be chosen to specify a particular type of telefunctioning. Here, telefunctioning is framed mathematically in terms of relationships which are independent of

[1] C. L. Moore is currently working at the NASA Langley Research Center.

[2] In this article, the word *environment* represents any object being manipulated or pushed by the slave robot.

[3] Describing the history and background of telerobotic control methods requires familiarity with the nomenclature and modeling approach used to describe telefunctioning. Thus, the history and background of telerobotic control methods is given later (Section 4).

[4] The subscript "M" signifies the master and "S" signifies the slave. Unless otherwise noted, all variables are defined in the Laplace domain. The Laplace arguments for all functions are omitted.

Contributed by the Dynamic Systems and Control Division for publication in the JOURNAL OF DYNAMIC SYSTEMS, MEASUREMENT, AND CONTROL. Manuscript received by the Dynamic Systems and Control Division May 24, 1990. Associate Technical Editor: W. Book.

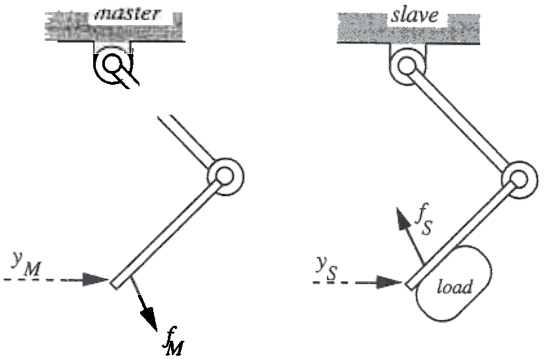

Fig. 1 In telerobotic system, human constrains master robot motion while environment constrains slave robot motion

the chosen control techniques. Without formal proof[5], it is stated that, for linear systems, only three independent relationships can be specified among the four variables: y_S, y_M, f_S, and f_M. One logical and possible set of relationships is:

$$y_S = A_y y_M \tag{1}$$

$$f_S = A_f f_M \tag{2}$$

$$f_S = Z_S y_S \tag{3}$$

A_y, A_f, and Z_S are transfer functions. A_y and A_f represent the relationships between the positions and forces while Z_S is the slave port impedance. Note that, once the above three relationships are specified, no other independent relationships can be specified. Figure 2 shows the variables and their relationships graphically where the thick lines represent the specified relationships (Eqs. (1), (2), and (3)) and the thin lines portray the dependent relationships.

Employing Eqs. (1), (2), and (3), the system dynamic behavior (i.e., the design specifications for telefunctioning) in example 1 can be expressed by the following equations:

$$A_f = -\alpha \tag{4}$$

$$A_y = 1 \tag{5}$$

$$Z_S = \text{arbitrary}. \tag{6}$$

A_f in Eq. (4) is the force amplification, and A_y in Eq. (5) states the equality of the master robot and slave robot positions. Equation (6) shows that designers can freely choose the slave port impedance, Z_S. Note that, once Eqs. (4), (5), and (6) are specified, no other equations can be specified for the system.

Applying Eqs. (1), (2), and (3) to example 2, the design specifications for telefunctioning become:

$$A_f = -1 \tag{7}$$

$$A_y = 1 \tag{8}$$

$$= ms \tag{9}$$

where m represents the desired mass and s is the Laplace operator. Substituting y_S and f_S from equations 1 and 2 into equation 3 and incorporating Eqs. (7), (8), and (9) yield a relationship between y_M and f_M such that $f_M = ms^2 y_M$. This equation proves that the human, when maneuvering a rigid body, would feel the forces due to maneuvering a single-point mass m.

A set of performance specifications for telefunctioning (e.g., Eqs. (1), (2), and (3)) does not assure system stability but does let designers express what they wish to have happen during a maneuver. If A_f and A_y are specified as "unity", then telepresence is seen to be a subclass of telefunctioning in which all the variables (e.g., position, velocity, force) of the master robot and the slave robot are dynamically equal. But, in telefunctioning, the dynamic behaviors of the slave robot and master robot are functions of each other; these functions are the designer's choice and depend on the application. Note that, although the design specifications described above are independent of the control architecture used, the next section introduces a new and practical control architecture to achieve these specifications and produce telefunctioning.

2 The Control Architecture

The control architecture which creates telefunctioning has the following properties.

1. It lets designers handle the robustness of the master robot and the slave robot without getting involved in the dynamics of the human, the dynamics of the object being manipulated by the slave, or the communication time delay [1]. Thus, designers can minimize the sensitivity of the master robot and the slave robot to uncertain dynamic modeling of each robot independent of other variables such as human and load dynamics.
2. This control architecture is the most general extension of the previous telerobotic control architectures[6] and allows choosing from a variety of performance specifications. This work shows how conveniently the design specifications in Section 1 can be mapped onto the variables of the proposed control architecture.
3. The human wearing the master robot is in physical contact with the machine, so *power transfer* is unavoidable and *information signals* from the human help to control both master robot and slave robot. The proposed control architecture conveniently depicts these two paths of human-machine interaction.

To clarify the proposed control law, the rich concepts of linear control theory are used for a single-degree-of-freedom telerobotic system. Understanding the proposed control approach requires understanding the dynamic behaviors of the master and slave robots, the human arm, and the environment, as discussed in the following subsections.

Dynamic Behaviors of the Master Robot and the Slave Robot. It is assumed that both the master robot and the slave robot primarily have independent closed-loop position controllers. The use of these primary stabilizing compensators[7] in both the master and the slave is motivated by the following reasons.

[5] Bond Graph Theory [18] can be used to prove that the system causality will be violated if more than three relationships are specified among the four variables y_S, y_M, f_S, and f_M. For the sake of brevity, this proof is not given here.

[6] A comparison between the previous telerobotic control methods and the control method presented in this paper is given in Section 4.

[7] Hereafter, the words *primary stabilizing compensators* refer to two closed-loop position controllers which stabilize the master robot and the slave robot. These controllers also decrease the effect of friction forces in the robots' joints.

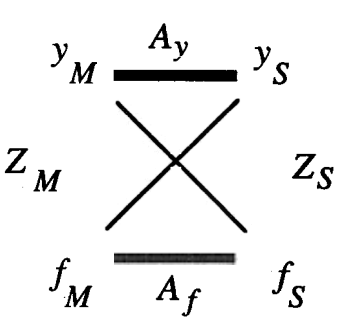

Fig. 2 If three relationships (thick lines) are specified among four variables, then other relationships (thin lines) depend on specified relationships

1. For the safety of the human, the master must remain stable when not worn by the human. A closed-loop position controller keeps the master stable when not worn by the human.
2. This controller also attenuates the effects of frictional forces in the joints and in the transmission mechanism, thus attenuating the sensitivity of each robot to uncertain forces.
3. The design of the primary stabilizing compensator lets the designers deal with the robustness of the master robot and the slave robot without getting involved in the dynamics of the human, the dynamics of the object being manipulated by the slave, or the communication time delay. A variety of robust control methods can be used to stabilize the master and slave robots independently. (Refer to [7, 19, 21] for two well-established robotic trajectory control techniques.)

Only the master dynamic behavior is derived here; the derivation of the dynamic behavior of the slave robot is similar to that of the master robot. The master robot position, y_M, results from two inputs: the electronic command to the primary controller of the master robot and the forces imposed on the master robot. The transfer function G_M is defined as the primary closed-loop system and has the electronic command u_M as input and the master position, y_M, as output. The master robot sensitivity transfer function, S_M, maps the force imposed on the master robot, f_M, onto the master position, y_M; S_M is the reciprocal of the robot stiffness. Equation (10) represents the master robot dynamic behavior in its most general form:

$$y_M = G_M u_M + S_M f_M \tag{10}$$

Since the master robot is in contact with only the human, f_M represents forces from only the human. The motion of the master robot has a small response to the human forces, f_M, if the magnitude of S_M is small. A small S_M is produced by use of a high-gain closed-loop positioning system as the primary controller or use of actuators with large gear ratios [10].

Similarly, the dynamic behavior of the slave robot is defined by Eq. (11):

$$y_S = G_S u_S + S_S f_S \tag{11}$$

f_S is the force imposed by the environment on the slave endpoint, and u_S is the input command to the primary controller of the slave drive system. G_S and S_S are similar to G_M and S_M, and represent the effects of u_S and f_S.

Dynamic Behavior of the Human Arm. The human arm dynamic behavior is modeled as a functional relationship between a set of inputs and a set of outputs. Therefore, the internal structures of the model components are not of concern; the particular dynamics of nerve conduction, muscle contraction, and central nervous system processing are accounted for implicitly in constructing the dynamic model of the human arm. (Refer to [12, 15, 17, 22] for a thorough review on various dynamic models of the human arm.)

In this work, the human arm is modeled as a nonideal force control system in which the force imposed by the human arm on the master robot results from two inputs. The first input, u_H, is issued by the human central nervous system; it is assumed that the specified form of u_H is not known other than it is human thought deciding to impose a force on the master robot. The second input is the position of the master robot. Thus, the master robot motion can be thought of as a position disturbance occurring on the force-controlled human arm. If the master robot is stationary, the force imposed on the master robot is a function of commands from the central nervous system only. If the master robot moves, the force imposed on the master robot is a function not only of the central nervous system commands but also of the master robot position, and the amount of force imposed on the master robot is different from u_H. The transfer function S_H maps the master robot position, y_M, into the force imposed on the master robot, f_M:

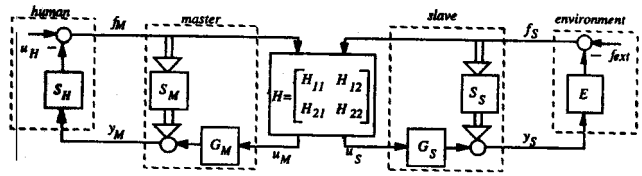

Fig. 3 Major elements of proposed control architecture which creates telefunctioning

$$f_M = u_H - S_H y_M \tag{12}$$

S_H, the human arm sensitivity function (or impedance [8, 11, 12]), is the disturbance rejection property of the human arm. If the gain of S_H is small, the master robot motion has a small effect on the imposed forces, f_M.

Dynamic Behavior of the Environment. Telerobotic systems are used for manipulating objects or imposing forces on objects. Defining E as a transfer function representing the environment dynamics and f_{ext} as the equivalent of all the external forces imposed on the environment, Eq. (13) provides a general expression for the force imposed on the slave robot in the linear domain[8]:

$$f_S = -E y_S + f_{ext} \tag{13}$$

If the slave robot is employed for pushing a spring and damper, then E is a transfer function such that $E(s) = (K + Cs)$ and $f_{ext} = 0$ where K, C, y_S, and s are the stiffness, damping, slave position, and Laplace operator. In another example, if the slave robot is employed for maneuvering a mass, then $E(s) = m_o s^2$ where m_o is the mass of the object.

The dynamic behavior of the telerobotic system, the human arm, and the environment is represented by the block diagram of Fig. 3 which uses Eqs. (10), (11), (12), and (13) as the dynamic models of the master robot, the slave robot, the human arm, and the environment. In the diagram, H is the control feedback operating on the contact forces. Note that there is no cross-feedback between the positions; only the forces are measured for feedback. This is a fundamental difference between this control method and previous control methods. (See Section 4 for a summary of previous telerobotic control methods.)

In Fig. 3, if u_S, u_M, u_H, and f_{ext} are zero (i.e., the inputs to the master robot and the slave robot are zero, the human has no intention of moving the master robot, and no other forces are imposed on the slave) and H_{11} and H_{21} are chosen to be zero, the interaction force between the human and the master is zero. If the human decides to move his hand (i.e., u_H becomes a nonzero value) and u_M, u_S, f_{ext}, H_{11}, and H_{21} are still zero, a small master motion develops from the interaction force between the master and the human. The master motion is trivial if S_M has a small gain, even though the interaction force may not be small. In other words, the human arm may not have the strength to overcome the master primary control loop. To solve this problem, the interaction force f_M is measured and filtered by compensator H_{11} and then used as an input to the master robot's primary controller. Note that the mapping $G_M H_{11}$ acts in parallel to S_M and thus increases the apparent sensitivity of the master robot. At this point, there is no restriction placed on the structure and size of H_{11}, but Fig. 3 suggests choosing a

[8] f_{ext} can be thought as the equivalent of all the forces on the slave robot endpoint which do not depend on y_S and other system variables. One example of f_{ext} can be observed when a second human is holding and maneuvering the slave endpoint; the force imposed on the slave endpoint by the human represents f_{ext}. In this article it is assumed that $f_{ext} = 0$.

large gain for H_{11} to increase the apparent sensitivity of the master robot. The interaction force f_M is also used to drive the slave robot after passing through the compensator H_{21}. If $H_{11} = H_{21}$, the master and slave motion are the same.

Similarly, compensator H_{22} is chosen to generate compliancy in the slave robot in response to the forces, f_S, imposed on the slave robot endpoint [9, 14]. The interaction force f_S also affects the master robot as a force reflection after passing through the compensator H_{12}.

The goal is to find the H transfer function matrix such that the satisfaction of Eqs. (1), (2), and (3) is guaranteed for the system. But, designers do not have complete freedom in choosing the structure and magnitude of H because the closed-loop system must remain stable for any chosen H. The proposed controller creates a desired stable behavior for the master and slave based on the human arm and environment models generated by the computer. The output of this controller is then fed to both the master and slave drive systems. The master robot also interacts physically with the human; the master motion, then, is partially due to the transfer of human power via S_M (shown by double lines in Fig. 3) and partially due to the command generated by the computer via H. The slave robot interacts physically with the environment; its motion, then, is partially due to the transfer of power from the environment via S_S (shown by double lines) and partially due to the command generated by the computer via H. The command to the slave robot must be such that the total slave maneuver becomes a desired maneuver that the person could not achieve alone.

3 Stability Analysis

In designing the controller which creates telefunctioning, the design objective is to select H such that the achievement of the design specifications in Eqs. (1), (2), and (3) is guaranteed. Here is described a simple control method which applies when a linear differential equations govern the dynamic behavior of the system. Inspection of the block diagram of Fig. 3 results in the following equations:

$$A_y = \frac{y_S}{y_M} = \frac{p_{21}}{p_{11} + \Delta p E}, \tag{14}$$

$$A_f = \frac{f_S}{f_M} = -\frac{p_{21}E}{1 + p_{22}E}, \tag{15}$$

$$Z_M = \frac{f_M}{y_M} = \frac{1 + p_{22}E}{p_{11} + \Delta p E} \tag{16}$$

$$Z_S = \frac{f_S}{y_S} = \frac{1 + p_{11}S_H}{p_{22} + \Delta p S_H} \quad \text{when} \quad u_H = 0, \tag{17}$$

where:

$$p_{11} = G_M H_{12} + S_M, \tag{18}$$

$$p_{12} = G_M H_{12}, \tag{19}$$

$$p_{21} = G_S H_{21}, \tag{20}$$

$$p_{22} = G_S H_{22} + S_S, \tag{21}$$

$$\Delta p = p_{11}p_{22} - p_{12}p_{21}. \tag{22}$$

Simple inspection shows that Eqs. (14), (15), and (16) are not independent and that they satisfy the following equation:

$$\frac{A_y}{A_f} = -\frac{Z_M}{E} \tag{23}$$

Thus, once A_y and A_f are specified (via Eqs. (1) and (2)), the designer cannot choose Z_M arbitrarily; Z_M must be derived from Eq. (23). Therefore, the design specifications must include one arbitrary choice for Z_S and two choices from among the three variables A_y, A_f, and Z_M. (This confirms that only three relationships are necessary to describe the system behavior.) Here A_y, A_f, and Z_S are chosen as the design specifications[9] and three Eqs. (14), (15), and (17) are solved to calculate four unknowns p_{11}, p_{12}, p_{21}, and p_{22}. Since Eqs. (14), (15), and (17) contain four unknowns, arbitrary assignment of p_{11} leads to the following solutions for p_{12}, p_{21}, and p_{22}:

$$p_{12} = -\frac{A_f + A_y E p_{11}}{A_f A_y E} \tag{24}$$

$$p_{21} = -\frac{A_f A_y (1 + S_H p_{11})(E + Z_S)}{Z_S(A_y E - A_f S_H)} \tag{25}$$

$$p_{22} = \frac{A_y E^2 (1 + S_H p_{11}) + S_H Z_S (A_f + A_y E P_{11})}{E Z_S (A_y E - A_f S_H)} \tag{26}$$

Once p_{12}, p_{21}, and p_{22} are found from Eqs. (24), (25), and (26), members of H can be found from equations 18 through 21.

In the above method, designers have complete freedom to select Z_S, A_y, and A_f. However, the stability of the closed-loop system in Fig. 3 is not guaranteed for all possible values of Z_S, A_y, and A_f. Using the Nyquist stability criterion (Appendix A), it can be found that the following two conditions are needed to guarantee the stability of the closed-loop system shown in Fig. 3:

$$|P_{11}| < \frac{1}{|S_H|} \quad \text{for all} \quad \omega \in [0, \infty) \tag{27}$$

$$\left|\frac{1 + p_{11}S_H}{p_{22} + \Delta p S_H}\right| > |E| \quad \text{for all} \quad \omega \in [0, \infty) \tag{28}$$

Comparing inequality 28 with Eq. (17) shows that the left-hand side of Eq. (28) equals Z_S. To guarantee stability inequalities 27 and 28 must be satisfied: Z_S must be larger than E and p_{11} must be smaller than $1/S_H$ in magnitude. This presents an interesting property of the proposed control law: the stability criteria (inequalities 27 and 28) do not limit the designer in choosing A_y, and A_f, but only restrict the designers in choosing Z_S. Although the designer has flexibility in shaping the magnitude frequency response of the right hand side of inequalities 27 and 28, these sufficient conditions for stability are nevertheless very conservative. As shown in the example in Section 5, in certain cases, inequality 28 cannot be satisfied for high frequencies since E (the environment dynamics) approaches infinity at high frequencies and Z_S is not larger than E at high frequencies. When the environment dynamics does not approach infinity, then one might be able to satisfy the stability condition for all frequencies. To summarize, designers can choose three functions A_f, A_y, and Z_S to describe the system behavior; while there is no restriction on the choice of A_f and A_y, Z_S (slave impedance) must be larger than E to guarantee the system stability.

4 History and Background

Hannford categorizes present telerobotic control architectures into classical position error architecture and forward flow architecture [6] which are described here in terms of the nomenclature and modeling approach used to describe telefunctioning.

In position error architecture (Fig. 4), the master position is the reference input command to the slave primary control loop, and the slave position is the input command to the master primary control loop. In other words, the position error between the master and slave positions drives the robots. There is no force reflection since no forces are measured. However, a posi-

[9] Also, either A_y, Z_M, and Z_S, or A_f, Z_M, and Z_S can be chosen as the set of design specifications.

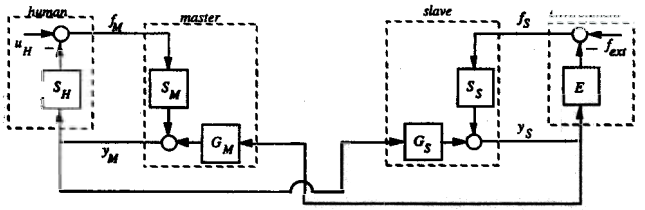

Fig. 4 Position error control architecture

tion error is generated whenever the slave robot contacts the environment, and this allows the human to feel the interaction. The main disadvantage of position error architecture is that the human must work against the impedance of the master robot. If the gain of S_M (defined in Eq. (10)) is small (i.e., large master impedance), then the human may not be able to exert sufficient force to move the robot. For this reason, position error architecture is best suited for use in direct-drive systems where the master impedance is relatively small. Another disadvantage of this architecture is its sensitivity to the communication time delay between the master and the slave which results from the feedback signal traveling in a long loop from the master to the slave and back again.

Forward flow architecture (Fig. 5) is similar to position error architecture in that the master position is used to drive the slave. Position information flows in the forward direction from the master to the slave, but the slave force is employed as the input command to the master primary control loop. Forward flow architecture is an improvement over position error architecture in that it provides true force reflection by sensing the force imposed on the slave robot. But forward flow architecture suffers from the same disadvantages as position error architecture; it does not permit adjustment of the master robot impedance, and it is sensitive to communication time delays.

Several researchers have noted that, in theory, local force feedback on the slave tends to improve stability [2, 5, 16]. A further enhancement can be made to the basic forward flow architecture if local force feedback is also utilized on the master. This increases the apparent sensitivity of the master robot to input commands from the human. In addition, it is conceptually desirable to have a symmetric system in which force information is communicated in both directions. Telefunctioning is the most general extension of these ideas. In this new architecture, both impedance and force amplification are modulated at both ends of the system.

5 Experiments

The one-degree-of-freedom telerobotic system shown in Fig. 6(a) is used to verify the performance of the system when the goal is to only amplify the force (i.e., example 1). As depicted in Fig. 6(b), the master robot is a link powered by a DC motor. The human holds the handle on the link to maneuver the master robot, and a force sensor between the handle and the link measures the human contact force. The slave robot is also a link powered by a DC motor. A mass representing a load is attached to the slave link, and a force sensor between the load and the link measures the load force. (The detailed drawings of the

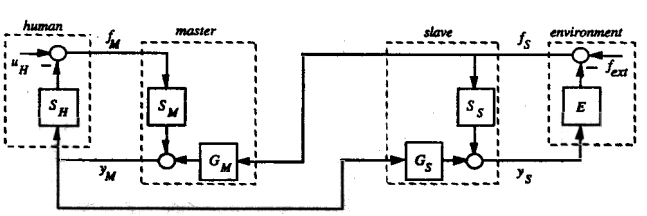

Fig. 5 Forward flow control architecture

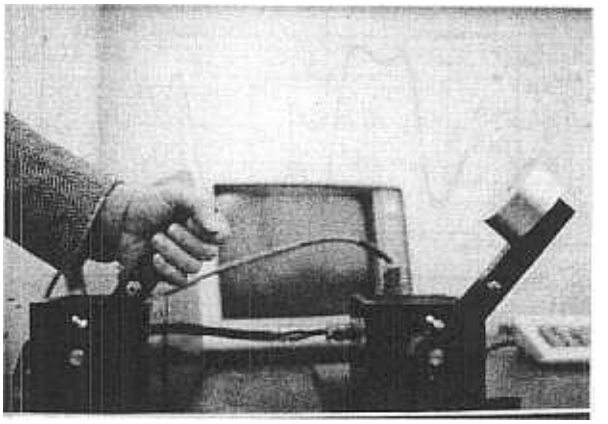

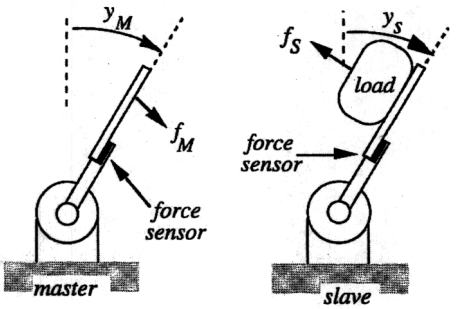

Fig. 6 One-degree-of-freedom telerobotic system

force sensor assembly have been omitted for brevity.) Two independent primary stabilizing controllers for the master robot and for the slave robot have been designed to yield the widest bandwidth for the closed-loop transfer functions, G_M and G_S, while guaranteeing the stability of each system in the presence of bounded unmodeled dynamics. The dominant dynamics for G_M, G_S, S_M, and S_S representing the closed-loop positioning system are given by Eqs. (29) through (32). (The development of the position controllers for both robots has been omitted for brevity; reference [4], however, gives a thorough description of these motor controllers.)

$$G_M = \frac{0.95}{0.1s + 1} \quad \text{rad/rad} \tag{29}$$

$$G_S = \frac{0.9}{0.05s + 1} \quad \text{rad/rad}$$

$$S_M = \frac{0.03}{0.1s + 1} \quad \text{rad/lbf} \tag{31}$$

$$S_S = \frac{0.05}{0.05s + 1} \quad \text{rad.lbf}$$

The master robot's bandwidth is about 10 rad/sec while the slave's bandwidth is about 20 rad/s. Since G_M and G_S transform position commands to actual robot positions, their units are rad/rad. Transfer functions S_M and S_S represent the sensitivity of each system to forces; their units are rad/lbf.

The model derived for the human arm holding the master robot does not represent the human arm sensitivity S_H for all configurations; it is only an approximate and experimentally verified model of the author's elbow in the neighborhood of the Fig. 4 configuration when the master robot deviation from the vertical is small. For the experiment which determines S_H, the human holds the handle, and the master is commanded to oscillate via sinusoidal functions. At each frequency of the master robot oscillation, the human tries to move his hand to follow

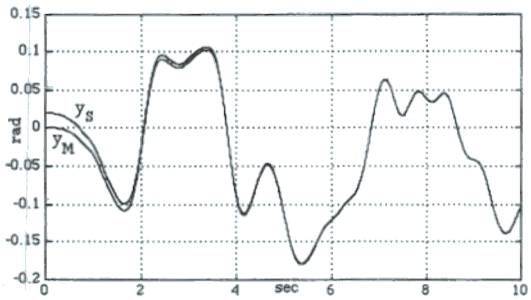

Fig. 7 Master and slave positions

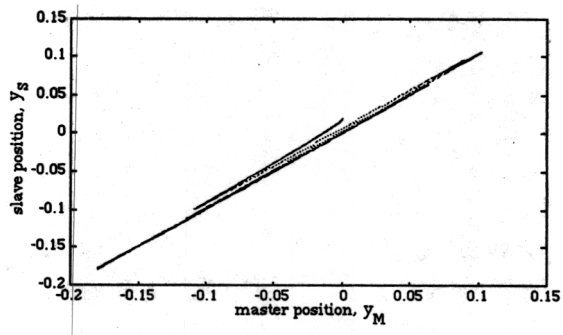

Fig. 8 Slave position versus master position

the master so that zero contact force is created between his hand and the master robot. Since the human arm trying to create contact forces cannot keep up with the high frequency motion of the master, large contact forces and consequently, a large S_H is expected at high frequencies. Since this force is equal to the product of the master robot acceleration and human arm inertia (Newton's second law), at least a second-order transfer function is expected for S_H at high frequencies. On the other hand, at low frequencies (in particular at DC), the human can comfortably follow the master robot motion, and thus always establish almost constant contact forces between his hand and the master robot. This leads to the assumption of a constant transfer function for S_H at low frequencies where contact forces are small for all values of the master robot position. Based on several experiments, at various frequencies, an estimate for the human's arm sensitivity is given in [11]. Equation (33) represents an approximation of the human arm dynamics in the neighborhood of the Fig. 4 configuration when the master robot deviation from the vertical is small:

$$S_H = 2.4(s + 1) \quad \text{lbf/rad} \tag{33}$$

The slave robot is employed to maneuver a mass with an inertia such that:

$$E = 10s^2 \quad \text{lbf/rad.} \tag{34}$$

The objective of the experiment is to design the H matrix such that the human feels $\frac{1}{5}$ of the force imposed on the slave while the master and slave positions are equal: $A_f = 5$ and $A_y = 1$. p_{11} is chosen to be $|1/[5(1 + s)^2]|$ satisfying inequality 27. Z_M is chosen to be 2.2 s^2 experimentally for operator comfort. Substituting the above values into Eqs. (24), (25), and (26) results in transfer functions for p_{12}, p_{21}, and p_{22} and the H matrix from Eqs. (18) through (21):

$$H_{11} = \frac{-1.5s^2 - 2s + 8.5}{47.5(s + 1)^2} \tag{35}$$

$$H_{12} = \frac{(s + 10)(7s^2 + 10s + 5)}{475s^2(s + 1)^2} \tag{36}$$

$$H_{21} = 0.3182\,\frac{(s + 20)}{(s + 0.5279)(s + 9.4721)} \tag{37}$$

$$H_{22} = -\frac{(s + 3.12)(s + 7.43)(s^2 + 0.687s + 0.43)}{18s^2(s + 0.5279)(s + 9.4721)} \tag{38}$$

The system is then maneuvered irregularly by an operator for 10 seconds. The motion generated by the operator can be thought of as a random function with low frequency components which fall within the bandwidth of the system. Figure 7 shows that the initial position of the master robot differs from the initial position of the slave robot; the master and slave positions, y_M and y_S, approach each other after the initial transition period. Figure 8 represents the slave position versus the master position where the approximately unity slope confirms the equality of master and slave positions for all low frequency components of the motion. Figure 9 depicts the master and slave forces for the same maneuver where the forces are initially equal; after the initial transition period, the master force, f_M, becomes five times less than the slave force, f_S. ($-f_S$ is plotted in this figure to indicate the opposite directions of f_M and f_S originating from the convention in Fig. 1). Figure 10 shows $-f_S$ versus f_M where the slope of 5 confirms that the operator feels 20 percent of the slave force.

Substitution of all parameters into inequality 28 reveals this inequality cannot be satisfied at high frequencies although the system has exhibited to be stable throughout maneuvers shown here. Inequality 28 is only a sufficient condition for stability (and consequently a conservative one). If this inequality is satisfied, the closed-loop stability is strongly guaranteed, however when this inequality is not satisfied (as in the case described here), no conclusion can be drawn. It is our hope that this bottleneck can be worked out through further research.

6 Summary and Conclusion

This article introduces robotic telefunctioning. Telefunctioning facilitates maneuvering of loads by creating a perpetual

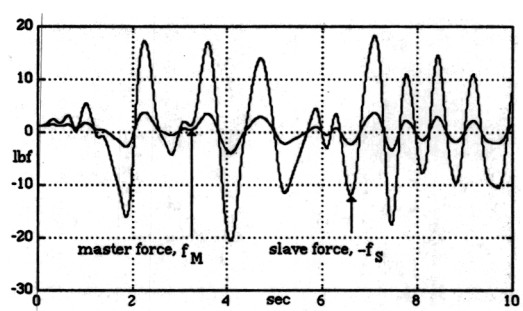

Fig. 9 Slave force is five times larger than master force

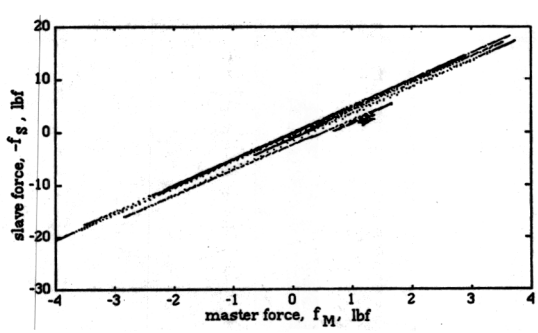

Fig. 10 Slave force versus master force

sense of the load dynamics for the operator. A minimum number of functions are defined to frame the telefunctioning specifications. The stability of the system (i.e., master robot, slave robot, human, and the load being manipulated) is analyzed and sufficient conditions for stability are derived. A set of experimental results are given to verify the theoretical claims when force amplification is required for the system.

References

1 Anderson, R. J., and Spong, M. W., "Asymptotic Stability for Force Reflecting Teleoperators with Time Delay", IEEE Int. Conf. on Robotics and Automation, Scottsdale, AZ, May 1989.

2 Bejczy, A. K., and Handlykken, M., "Experimental Results with a Six Degree-of-Freedom Force Reflecting Hand Controller," *Proc. 17th Annual Conference on Manual Control*, Los Angeles, CA, June 1981.

3 Bejczy, A. K., Bekey, G., and Lee, S. K., "Computer Control of Space Borne Teleoperators with Sensory Feedback," IEEE Conference on Robotics and Automation, 1985.

4 *DC Motors, Speed Controls, Servo Systems*, Electro-Craft Corporation, Minnesota, 1980.

5 Hannaford, B., "A Design Framework for Teleoperators with Kinematic Feedback," *IEEE Trans. on Robotics and Automation*, Vol. 5, No 4, Aug. 1989.

6 Hannaford, B. "Stability and Performance Tradeoffs in Bilateral Telemanipulations," IEEE Int. Conference on Robotics and Automation, Scottsdale, AZ, May 1989.

7 Ha, I., Gilbert, E., "Robust Tracking in Nonlinear Systems and its Applications to Robotics", IEEE Conference on Robotics and Automation, San Francisco, CA, April 1986.

8 Kazerooni, H., and Guo, J., "Human Extenders," ASME JOURNAL OF DYNAMIC SYSTEMS, MEASUREMENTS, AND CONTROL, Vol. 115, No. 2(B), June 1993.

9 Kazerooni, H., and Waibel, B. J., "On the Stability of the Constrained Robotic Maneuvers in the Presence of Modeling Uncertainties," *IEEE Transactions on Robotics and Automation*, Vol. 7, No. 1, February 1991.

10 Kazerooni, H., "On the Robot Compliant Motion Control," ASME JOURNAL OF DYNAMIC SYSTEMS, MEASUREMENT, AND CONTROL, Vol. 111, No. 3, Sept. 1989.

11 Kazerooni, H., "Human-Robot Interaction via the Transfer of Power and Information Signals," *IEEE Trans. on Systems and Cybernetics*, Vol. 20, No 2, Mar. 1990.

12 Kazerooni, H., and Snyder, T. J., "A Case Study on Dynamics of Haptic Devices: Human Induced Instability in Powered Hand Controllers," *AIAA Journal of Guidance, Control, and Dynamics*, Vol. 18, No. 1, 1995

13 Lehtomaki, N. A., Sandell, N. R., and Athans, M., "Robustness Results in Linear-Quadratic Gaussian Based Multivariable Control Designs," *IEEE Trans. on Automatic Control*, AC-26(1):75–92, Feb. 1981.

14 Mason, M. T., "Compliance and Force Control for Computer controlled Manipulators," *IEEE Transactions on Systems, Man and Cybernetics SMC-*11(6):418–432, June 1981.

15 Rabischong, P., "Robotics for the Handicapped," *Proc. IFAC Symposium*, Columbus, OH, May 1982.

16 Raju, G. J., Verghese, G. C., and Sheridan, T. B., "Design Issues in 2-port Network Models of Bilateral Remote Manipulation," IEEE Int. Conference on Robotics and Automation, Scottsdale, AZ, May 1989.

17 Repperger, D. W., and Morris, A., "Discriminant Analysis of Changes in Human Muscle Function When Interacting with an Assistive Aid," *IEEE Transactions on Biomedical Engineering*, Vol 35, No 5, May 1988.

18 Rosenberg, R. C., and Karnopp, D. C., *Introduction to Physical System Dynamics*, McGraw-Hill, New York, NY, 1983.

19 Slotine J.-J. E., "The Robust Control of Robot Manipulators," *Int. J. of Robotics Res.*, Vol 4, No 2, 1985.

20 Sheridan, T. B., "Telerobotics", *Proceedings of the Workshop on Shared Autonomous and Teleoperated Manipulator Control*, Philadelphia, PA, 1988.

21 Spong, M. W., and Vidyasagar, M., "Robust Non-Linear Control of Robot Manipulators," *IEEE, Conference on Decision and Control*, December 1985.

22 Stein, R. B., "What muscles Variables Does the Nervous System Control in Limb Movements?", *J. of the Behavioral and Brain Sciences*, Vol 5, pp 535–577, 1982.

APPENDIX A

A sufficient condition for stability of the closed-loop system in Fig. 3 is developed by the Nyquist Theorem [13]. This sufficient condition results in a class of compensators, H, which guarantee stability. Note that the stability condition derived in this section does not give any indication of system performance, but only ensures a stable system.

After some manipulation, the block diagram of Fig. 3 can be represented by the block diagram of Fig. A1. Note that there are two elements in the feedback loop: RQ represents the natural feedback loops which occur as a result of human-master interaction and environment-slave interaction, and RGH represents the controlled feedback loop. An assumption is made that the system in Fig. A1 is stable when $H = 0$. If the controller in the feedback loop is eliminated by setting $H = 0$, the system reduces to the case where the human wears the master robot and the slave is in contact with the environment, but command inputs to the primary controller of both robots are zero. The plan is to determine how robust the system is when H takes on a nonzero value. Specifically, the goal is to obtain a sufficient stability condition when H is added to the system. To achieve this, the Nyquist criterion is used. The following assumptions are made:

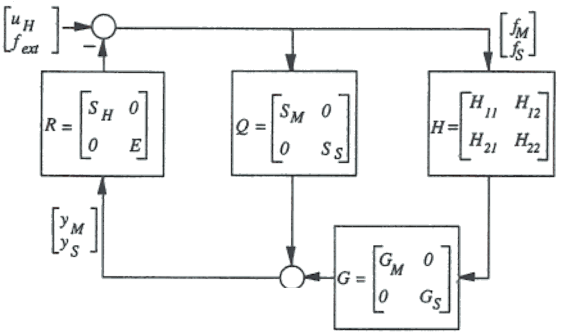

Fig. A1 Loop RQ represents human-master and environment-slave physical contact

1. The closed-loop system in Fig. A1 is stable when $H = 0$. This assumption states that the system of human and master robot taken as a whole and the system of environment and slave robot taken as a whole remain stable when no feedback compensator H is used in the system.

2. H is populated with stable linear transfer functions. Therefore, the loop transfer function, RQ, has the same number of right half-plane poles as $(RQ + RGH)$.

For convenience in this stability analysis, it is assumed that $A = RQ$ and $B = (RQ + RGH)$. According to the Nyquist criterion, the system in Fig. A1 remains stable as long as the number of anti-clockwise encirclements of det $(I + B)$ around the origin of the s-plane is equal to the number of unstable poles of the loop transfer function B. By assumptions 1 and 2, B and A have the same number of unstable poles. Assuming that the system is stable when $H = 0$, the number of encirclements of the origin by det $(I + A)$ is equal to the number of unstable poles in A. When compensator H is added to the system, the number of encirclements of the origin by det $(I + B)$ must be equal to the number of unstable poles in B in order to guarantee closed-loop stability. Because of the assumption that the number of unstable poles in B and A is identical, det $(I + B)$ must have exactly the same number of encirclements of the origin as det $(I + A)$. In order to guarantee equal encirclements by det $(I + A)$ and det $(I + B)$, insurance is needed so det $(I + B)$ does not pass through the origin of the s-plane for all frequencies.

$$\det(I + RQ + RGH) \neq 0 \quad \text{for all} \quad \omega \in [0, \infty) \quad \text{(A1)}$$

Substituting R, Q, G, and H from Fig. A1 into Eq. (A1) and calculating the determinant results in:

$$S_H E \Delta p + p_{22} E + S_H P_{11} + 1 \neq 0 \text{ for all } \omega \in [0, \infty) \quad \text{(A2)}$$

$$\text{if} \quad S_H p_{11} + 1 \neq 0 \quad \text{for all} \quad \omega \in [0, \infty) \quad \text{(A3)}$$

Then, dividing (A2) by (A3) results in:

$$1 + \frac{(S_H \Delta p + p_{22})E}{S_H p_{11} + 1} \neq 0 \quad \text{for all} \quad \omega \in [0, \infty) \quad \text{(A4)}$$

To ensure the truth of (A4), one must guarantee that:

$$\left|\frac{(S_H \Delta p + p_{22})E}{S_H p_{11} + 1}\right| < \quad \text{for all} \quad \omega \in [0, \infty) \qquad \text{(A5)}$$

$$\left|\frac{1 + p_{11} S_H}{p_{22} + \Delta p S_H}\right| > |E| \quad \text{for all} \quad \omega \in [0, \infty) \qquad \text{(A6)}$$

Therefore, to ensure the stability of the system in Fig. A1, inequalities (A5) and (A3) must be guaranteed; these inequalities are restated as follows:

$$|p_{11}| < \frac{1}{S_H} \quad \text{for all} \quad \omega \in [0, \infty) \qquad \text{(A7)}$$